RSC Advances

This is an *Accepted Manuscript*, which has been through the Royal Society of Chemistry peer review process and has been accepted for publication.

Accepted Manuscripts are published online shortly after acceptance, before technical editing, formatting and proof reading. Using this free service, authors can make their results available to the community, in citable form, before we publish the edited article. This *Accepted Manuscript* will be replaced by the edited, formatted and paginated article as soon as this is available.

You can find more information about *Accepted Manuscripts* in the Information for Authors.

Please note that technical editing may introduce minor changes to the text and/or graphics, which may alter content. The journal's standard Terms & Conditions and the Ethical guidelines still apply. In no event shall the Royal Society of Chemistry be held responsible for any errors or omissions in this *Accepted Manuscript* or any consequences arising from the use of any information it contains.

ROYAL SOCIETY OF CHEMISTRY

www.rsc.org/advances

Tuning of Photoluminescence Properties and Ultrasensitive Trace Detection in Few Layers MoS_2 by the Decoration of Gold Nanoparticles

Shib Shankar Singha[a], Dipanjan Nandi[a], Achintya Singha[a*]

[a] Department of Physics, Bose Institute, 93/1, Acharya Prafulla Chandra Road, Kolkata 700 009, India.

* To whom correspondence should be addressed: E-mail: achintya@jcbose.ac.in, Phone: + 91 33 23031177, Fax: + 91 33 23506790

RSC Advances Accepted Manuscript

ABSTRACT

We report an easy and inexpensive chemical route for the decoration of few layers MoS_2 with Au nanoparticles (NPs). The Au-NPs are formed on the defective sites of the MoS_2 and localized by non-covalent bond. The NPs act as p-type dopant in MoS_2 layer. An enhancement of the photoluminescence (PL) intensity of the Au-MoS_2 composite with respect to bare few layers MoS_2 has been observed. We also systematically observed blue shift of the excitonic emission as the number and size of the Au-NPs on MoS_2 increases. Both the phenomena have been understood by switching between charged exciton (trion) recombination and neutral exciton recombination. The application aspects of the Au-MoS_2 composite have been demonstrated by using it as a substrate for surface-enhanced Raman scattering (SERS). The SERS measurements show a uniform, reproducible, and strong Raman signal from the adsorbed molecules with concentration down to 10^{-12} M. Our results provide a method to tune the optical and electronic properties of MoS_2 and the Au-MoS_2 composite might be useful as an efficient SERS substrate for the ultrasensitive detection of biomolecules.

Keywords: Au-MoS_2 hybrid structure, tuning of photoluminescence properties, Raman study, SERS, high enhancement factor.

RSC Advances Accepted Manuscript

Introduction:

Layered transition-metal dichalcogenides (LTMDs) have been drawn attention in recent years due to its flamboyant optoelectronic properties.[1-3] LTMDs are represented by a general formula of MX_2 where, M is IVB, VB or VIB transition metal and X is sulphur, selenium, or tellurium.[4] MoS_2 are belonging to the family of LTMDs. Being a zero bandgap material; pristine graphene invokes a constraint on uses of it in visible range of frequencies .[5] In MoS_2, Mo layer is sandwiched between two hexagonal S layers. The atomic layers of MoS_2 are held together by weak van der Waals force and due to this reason; layers can be exfoliated very easily with different techniques. Monolayer MoS_2 is a direct bandgap semiconductor of energy ~1.9 eV[3,6,7], due to which it shows strong photoluminescence.[1,8] Therefore, monolayer MoS_2 has been used in several optoelectronic applications such as, interband tunnel field effect transistors (FETs),[9] photodetectors,[10-12] photovoltaics [13-15] and light emitters.[3,16] In mono/few layers MoS_2, due to the presence of strong Coulomb interactions optically generated electron–hole pair form stable exciton states even at room temperature.[17,18] Therefore, the carrier density has an important role in the optical properties of mono/few layers MoS_2. Doping is one of the effective techniques to control the carrier density of the monolayer TMDs.[17-21] Among different doping methods such as application of gate bias voltage using a FET device,[18-20] gas physisorption [21] etc; chemical doping is a simpler, cheaper and convenient technique for controlling the carrier density of layered materials.[17,22,23] Mouri *et al.* [17] have shown an enhancement and reduction of PL intensity when monolayer MoS_2 is chemically doped by p-type and n-type dopant, respectively.[17] It has also been reported that the Au-NPs attached at the edge sites of monolayer MoS_2 act as p type dopant.[24,25] However, Bhanu *et al.* [25] have observed quenching of PL in Au-MoS_2 hybrid structure, which is inconsistent with the result published in Ref.17. To understand the

RSC Advances Accepted Manuscript

optoelectronic properties and their consecutive application of MoS_2 and Au decorated MoS_2 requires a careful investigation on their structure.

In this work, few layers MoS_2 has been prepared from the bulk MoS_2 material by well known micromechanical cleavage or "scotch tape" method.[1,26,27] A 0D-2D composite structure has been synthesized by immersing the MoS_2 into $HAuCl_4$ solution. The Au-NPs (0D) are formed at the defective sites of MoS_2 (2D) and the number and size of the Au-NPs increase with the increase of immerging time. The intensity of the excitonic emissions are enhanced as the Au-NPs start growing on the MoS_2 layer. This observation has been attibuted to the fact that the Au-NPs act as p type dopant which reduces the intrinsic electrons in the bare sample yields an increase of exciton recombination. In addition to that the excitonic emission energy of composite system are blue shifted compared to the bare MoS_2, which is due to the increase of Fermi energy by the dissociation of charged exciton (trion). Stiffening of E^1_{2g} and softening of A_{1g} Raman modes with the increase in immerging time has been observed which is consistent with an earlier report.[28] The potential applicability of the Au-MoS_2 hybrid structure has been examined by using it as an surface enhanced Raman scattering (SERS) substrate. A uniform and reproducible SERS signals have been observed up to a 10^{-12} M concentration of Rhodamine 6G (R6G) dye. The enhancement factor we have achieved is sufficient to detect a single molecules. Hence, we conjecture that, the optical properties of few layers MoS_2 can be tuned by decoration of Au-NPs and the Au-MoS_2 hybrid structure can be utilized for ultrasensitive trace detection that might overcome the issues of low cross sections of Raman scattering.

RSC Advances Accepted Manuscript

Experimental Section

Reagents.

High purity bulk MoS_2 was purchased from SPI Suppliers, gold (III) chloride tetrahydrate ($HAuCl_4$, $4H_2O$) and Rhodamine 6G (R6G) were purchased from Sigma-Aldrich Pvt. Ltd. All chemicals were used as received without further purification. Mili-Q water was used during entire synthesis and experiments.

Preparation of Few layers MoS_2.

Few layers MoS_2 flake was prepared on the SiO_2 (300nm)/Si substrate by micromechanical exfoliation technique.[1,26] Before deposition of flake Si wafers were freshly cleaned by Piranha solution.

Preparation of Au-MoS_2 hybrid structure.

A 1 mM solution of $HAuCl_4$ was prepared by mixing proper amount of $HAuCl_4$ with mili pore water. Four different sets of sample were prepared by just varying the immerging time of MoS_2 flake containing SiO_2/Si substrate into $HAuCl_4$ solution for 30 min, 60 min, 90 min and 120 min and those samples were marked as S1, S2, S3 and S4, respectively.

Preparation of SERS substrate.

A Stock solution (10^{-3}M) of R6G was prepared with desired volume of water and stored in a cold place. Wide range of solutions having different concentration of R6G from 10^{-5} to 10^{-12} M was prepared from stock solution. The Sample S4 was used as SERS substrate. The sample was immersed into R6G solution for two hours and then rinsed with Mili-Q water and then dried with nitrogen flow. Finally, we have performed SERS measurements on this dye adsorbed substrates. The same procedure has been followed for all other concentration of R6G solutions.

RSC Advances Accepted Manuscript

Instruments used for various characterizations.

SEM analysis was done using model FEI, Quanta 200 with an accelerating voltage of 30kV.The Raman and PL measurements were performed using a micro Raman set up consisting of spectrometer (Lab RAM HR Jovin Yvon) and a Peltier cold CCD detector. An air cooled argon-ion laser (Ar^+) with wavelength 488 nm and diode laser of wave length 785 nm were used as excitation light source and a 100X objective with numerical aperture (NA) of 0.9 was used to focus the laser on the sample and to collect the scattered light from the sample.

Results and Discussions

Figure 1(a) shows the optical microscope image of the MoS_2 flake on SiO_2/Si substrate. The optical image has been taken using 100X objective. The contrast in the area of the image marked by red circle indicates that the few layers of MoS_2 are present at that region. The number of layers has been confirmed by Raman spectroscopy. Raman spectrum of the sample has been displayed in Figure 1(b). For reference we have also presented the Raman spectrum of bulk MoS_2. In MoS_2, E^1_{2g} phonon mode is originated due to the displacement of Mo and S atoms in the basal plane, whereas A_{1g} phonon mode is due to the vibration of S atom in opposite direction, along the perpendicular to the basal plane (see inset of Figure 1(b). The peak positions of the E^1_{2g} and A_{1g} modes are obtained from the fitting of experimental curve using two Lorenzian functions. The Raman modes are highly sensitive to the thickness of the layer.[27] In general, the gap between E^1_{2g} and A_{1g} peaks decreases as the number of layers decreases.[27] The gap for our MoS_2 layer is found to be 24.97 cm^{-1}, which ensures that the number of layers is less than 6.[27] We have also performed PL measurements for further confirmation of the layer number. Figure 1(c) shows the PL spectra of bulk MoS_2 (orange curve) and few layers MoS_2 (black curve). The large spin-orbit interaction in the few

RSC Advances Accepted Manuscript

layers MoS_2 splits the highest valance band located at the K point of the Brillouin zone. Therefore, the direct optical transitions from the top of the spin-split valance bands to the bottom of the conduction band give A1 and B1 peaks.[1] Both the peaks are associated with exciton recombination. In addition to that, PL peak of negative exciton (X^-, trion) is also present in micromechanical exfoliated MoS_2 layer, because, the layer unintentionally becomes n-type due to defects or substrate effect.[17,18,29] Therefore, we have fitted the PL spectrum using three Gaussian functions and the peak positions are at 1.80 eV, 1.86 eV and 1.96 eV corresponding to X^-, A1 and B1, respectively. The energy gap between X^- and A1 is ~60 meV, which is consistent with the value reported for mono layer MoS_2.[17,18,29] The intensity ratio of A1 and B1 is ~1.3, which is close agreement with reported value for 4 layers MoS_2,[25] corroborates the number of layers in our material is less than 6 as obtained from Raman measurements.

Scanning Electron Microscope (SEM) images of Au-MoS_2 hybrid structures (S2 and S4) are shown in Figures 2(a) and (b), respectively. From the SEM images it is clear that the number and size of Au-NPs are higher in S4 compared to S2 and no Au-NPs are observed on bare SiO_2 substrate. In MoS_2, defective sites are more reactive.[24] The $AuCl_4^-$ ions in the solution initially attract by the defective sites of the MoS_2 and act as nucleation centre for growth of Au particles.[24] So, with the increase of immerging time the number and dimension of the Au-NPs increase as observed in SEM images.

To investigate the role of Au agglomeration on MoS_2, PL measurement has been performed on Au-MoS_2 hybrid structure with excitation wavelength of 488 nm. Figure 3 shows the PL spectra of undoped MoS_2 (black), S1 (red), S2 (blue), S3 (magenta) and S4 (dark yellow) samples. All the spectra have been fitted with three Gaussian functions (for X^-, A1 and B1). Figure 3(b) shows the integrated intensity of the PL peaks as a function of

RSC Advances Accepted Manuscript

immerging time of MoS_2 inside the $HAuCl_4$. In the as-prepared sample the PL intensity is higher for trion (X^-) at energy 1.80 eV than the excitonic emission. This is because as-prepared MoS_2 unintentionally becomes n-type due to defects or substrate effect [18,29,30] where trion recombination is dominant and the result is consistent with the earlier reports.[17] The intensity of the neutral excitonic peaks increase monotonically up to immerging time of 60 min (sample: S3) and then mitigates, whereas the integral intensity of the trion peak remains almost constant. The experimental results are also consistent with earlier reports.[17] This behaviour can be attributed to the fact that in presence of Au-NPs the electronic structure of MoS_2 has been modified. Due to the difference of Fermi energy between MoS_2 (4.7 eV) [25]and Au (5.1 eV),[25] a band bending takes place in Au-MoS_2 hybrid structure. Upon illumination with a photon of appropriate energy the electron in the excited states of MoS_2 transfer to Au leaving behind a hole, which acts as p-dopant in MoS_2. As a result, the excess carrier in the MoS_2 layer decreases and the excitons recombination became predominant than the formation of trion. Moreover, the trions dissociate to excitons and one of the two electrons in the trion is unbound and placed at the Fermi level of the MoS_2 .[18] Therefore, the number of exciton increases with the increase of dipping time, yields the enhancement of intensity of the excitonic emission. Beyond 60 min, the PL intensity decreases because of the excess p doping. Figure 3(c) shows the PL energy shifts towards higher energy with the increase of immerging time of MoS_2 into the $HAuCl_4$ solution. As the exciton binding energy is large,[18] neutral excitons emit higher energy than trion. The increased number of neutral excitons yields the PL energy shift.[29] The relative concentration of charged to neutral excitons can be estimated by the following expression.[17,18, 29]

$$\gamma = I_X^- / (I_X^0 + I_X^-)$$

RSC Advances Accepted Manuscript

where, I_i is the emission intensity of neutral or charged excitons (X^0 or X^-). The estimated values of γ are 0.63, 0.43, 0.16, 0.33 and 0.45 for as-prepared few layers MoS_2, S1, S2, S3 and S4, respectively. The experimental observation reflects that, lower value of γ contributes the intensity enhancement and blue shift of excitonic PL emission.

To enlighten how the adsorbed Au-NPs create impacts on the vibrational mode, Raman measurements have been performed on Au-MoS_2 hybrid structures. Figure 4(a) shows the Raman spectra of all the samples including as prepared MoS_2. The positions of E^1_{2g} and A_{1g} modes as a function of immerging time of MoS_2 into the $HAuCl_4$ solution are displayed in Figure 4(b). The A_{1g} mode shows a strong dependence on the dipping time as the carrier concentration changes with dipping time whereas E^1_{2g} shows less dependence on the carrier concentration. We have observed softening and broadening of the A_{1g} phonon mode as we increase the immerging time, which is due to the interaction of plasmon with A_{1g} phonon**.** The maximum shift of A_{1g} mode is found to be 4 cm^{-1}, which is consistent with electron doped single layer MoS_2 by Chakraborty *et al.*[28]

To explore the utility of the metal-semiconductor composite system as an ultrasensitive trace detection, the Au-MoS_2 hybrid structure have been used as a substrate for surface enhanced Raman spectroscopy (SERS) study. The two well known effects that are involved in SERS; chemical and electromagnetic mechanism (EM) effects. The chemical effect is originated due to the charge transfer between metal nanostructure and the molecule adsorbed at the metal surface. The localized electromagnetic field, originating from the resonant coupling of the incident light with surface plasmons is the origin of EM effect. The EM effect dominates to enhance the Raman signal in the SERS phenomenon.[31-38] The plasmonic coupling effects at the inter particle gap in a cluster of noble-metal particles provide an intensively localized electromagnetic field which is known as hot spots. The Raman active molecules adsorbed at the hot spots can be detected at single-molecule

RSC Advances Accepted Manuscript

level.[31,39-46] A lot of efforts have been focused on the preparation of stable metal clusters with narrow inter particle gaps. DNA has been widely employed as a scaffold to produce specifically dispersed metal nanoparticles and to control the locations of these particles .[47-52] Recently, metal nanoparticles decorated graphene and graphene oxide have been used as efficient SERS substrate to detect molecules with nM concentration level.[53] In the present work, the Au-NPs are tightly immobilized by MoS_2 and provide the abundant hot spots. R6G has been used as a Raman probe molecule. The normal Raman spectrum of solid R6G dye is presented in Figure 5. The characteristic bands of R6G are observed at 609, 775, 1187, 1305, 1360, 1506, 1572 and 1648 cm^{-1}. Peaks at 609 and 775 cm^{-1} are due to in plane xanthene ring deformation and out of plane C-H bend, respectively.[54] The mode at 1187, 1305 and 1360 cm^{-1} are due to the in plane xanthene ring deformation (C-H bend, N-H bend), the in plane xanthen ring breathing (N-H bend, CH_2 wag) and in plane xanthene ring stretching (C-H bend), respectively.[54] The bands at 1506, 1572 and 1648 cm^{-1} are related to in plane xanthen ring stretching (C-H bend, N-H bend), in plane xanthene ring stretching (N-H bend) and in plane xanthene ring stretching (C-H bend), respectively .[54]

The SERS measurements have been performed using S4 sample with R6G solutions having concentrations of 1×10^{-5} , 1×10^{-6}, 1×10^{-9}, and 1×10^{-12} M. The SERS spectra at various concentrations recorded with 488 nm and 785 nm laser are shown in Figures 6 (a) and (b), respectively. The normal Raman spectrum of R6G with 1mM concentration (black curve) does not show any Raman band. But, Raman modes of R6G molecules on Au-Mos_2 substrate are clearly visible up to 10^{-12} M concentration level. The enhancement is higher for 488 nm laser than 785 nm laser, which is expected because 785 nm laser is far from plasmon resonance of Au-NPs. To get a quantitative idea of enhancement strength, the enhancement factor (EF) has been calculated from the experimental data. The estimated value of EF for the modes at 609, 1358, 1575 and 1648 cm^{-1} is ~10^{10}, which is sufficient to detect single

RSC Advances Accepted Manuscript

molecules.[52] We strongly believe that, in future the Au-MoS_2 hybrid structure will be useful for ultrasensitive detection of biomolecules and other technologically important fields.

Conclusions

In summary, we have presented a simple technique to realize 0D-2D hybrid structure in few layers MoS_2. The Au-NPs in this hybrid structure exhibit p-doping effect to the MoS_2. The hybrid structure has been studied systematically by PL and Raman measurements. We have demonstrated that the number and size of the Au-NPs play an important role to control the optical and vibrational properties of the MoS_2. The excitonic emission properties are highly modified in the presence of Au-NPs whereas the emission from trion is quite insensitive. The intensity and blue shift of the PL peaks have been understood by the conversion of trion to exciton under illumination of the hybrid structure. We have also shown that the E^1_{2g} phonon mode shows less dependence on the presence of Au-NPs compared to A_{1g} mode. Finally, we have utilized the hybrid structure as a potential SERS substrate for the detection at single molecule level. Hence, the Au-NPs decorated MoS_2 can provide hybrid nanomaterials for the application of future digital electronics and sensors.

RSC Advances Accepted Manuscript

References

1 A. Splendiani, L. Sun, Y. Zhang, T. Li, J. Kim, Y. C. Chim, G. Galli, and F. Wang, *Nano Lett.*, 2010, **10**, 1271–1275.

2 W. Zhao, Z. Ghorannevis, L. Chu, M. Toh, C. Kloc, P.- H. Tan, and G. Eda, *ACS Nano*, 2013, **7**, 1, 791-797.

3 K. F. Mak, C. Lee, J. Hone, J. Shan and T. F. Heinz, *Phy. Rev. Lett.,* 2010, **105**, 136805.

4 L. Yuwen, F. Xu, B. Xue, Z. Luo, Z. Qi, B. Bao, S. Su, L. Weng, W. Huang and L. Wang, *Nanoscale, The Royal Soc. of Chem.*, 2014, **6**, 5762–5769.

5 A. K. M. Newaz, D. P. J. I. Ziegler, D. Caudel, S. Robinson, R. F. Haglund Jr and K. I. Bolotin, *Solid State Comm.,* 2013, **155**, 49–52.

6 D. Gopalakrishnan, D. Damien and M. M. Shaijumon, *ACS Nano*, 2014, **8**, 5297–5303.

7 G. Eda, H. Yamaguchi, D. Voiry, T. Fujita, M. Chen and M. Chhowalla, *Nano Lett.*, 2011**,** **11**, 5111–5116.

8 S. Tongay, J. Suh, C. Ataca, W. Fan, A. Luce, J. S. Kang, J. Liu, C. Ko, R. Raghunathanan, J. Zhou, F. Ogletree, J. Li, J. C. Grossman and J. Wu, *Scientific Reports*., 2013, **3**, 2657.

9 S. Banerjee, W. Richardson, J. Coleman and A. Chatterjee, *IEEE Elect. Dev. Lett.,* 1987, **8**, 347-349.

10 Z. Yin, H. Li, L. Jiang, Y. Shi, Y. Sun, G. Lu, Q. Zhang, X. Chen and H. Zhang, *ACS Nano*, 2013, **6**, 74-80.

11 H. S. Lee, S.W. Min, Y.G. Chang, M. K. Park, T. Nam, H. Kim, J. H. Kim, S. Ryu, and S. lm, *Nano Lett.,* 2012, **12**, 3695−3700.

RSC Advances Accepted Manuscript

12 O. Lopez-Sanchezl, D. Lembke, M. Kayci, A. Radenovic, and A. Kis, *Nat. Nanotech.,* 2013, **8**, 497-501.

13 J. Feng, X. Qian, C.-W. Huang and J. Li, *Nature Photonics*, 2012, **6**, 866-872.

14 M. Fontana, T. Deppe, A. K. Boyd, M. Rinzan, A. Y. Liu, M. Paranjape and P. Barbara, *Scientific Reports***,** 2013, **3**, 1634.

15 M. Bernardi, M. Palummo and J. C. Grossman, *Nano Lett.***,** 2013, **13**, 3664−3670.

16 Y. Ye, Z. Ye, M. Gharghi, H. Zhu, M. Zhao, X. Yin and X. Zhang, *Applied Physics Letters*, 2014**, 104**, 193508.

17 S. Mouri, Y. Miyauchi and K. Matsuda, *Nano Lett.,* 2013, **13**, 5944-5948.

18 K. F. Mak, K. L. He, C. Lee, G. H. Lee, J. Hone, T. F. Heinz and J. Shan, *Nat. Materials,* 2013**, 12**, 207−211.

19 J. S. Ross, S. Wu, H. Yu, N. J. Ghimire, A. M. Jones, G. Aivazian, J. Yan, D. G. Mandrus, D. Xiao, W. Yao and X. Xu, *Nat. Comm.,* 2013**, 4**, 1474−1474.

20 A. M. Jones, H. Yu, N. J. Ghimire, S. Wu, G. Aicazian, J. S. Ross, B. Zhao, J. Yan, D. G. Mandrus, D. Xiao, W. Yao and X. Xu, *Nat. Nanotech.*, 2013, **8**, 634−638.

21 S. Tongay, J. Zhou, C. Ataca, J. Liu, J. S. Kang, T.S. Matthews, L. You, J. Li, J. C. Grossman and J. Q. Wu, *Nano Lett.,* 2013*,* **13**, 2831−2836.

22 W. Chen, S. Chen, D. C. Qi, X. Y. Gao and A. T. S. Wee, *J. Am.Chem. Soc.,* 2007, **129**, 10418−10422.

23 C. Coletti, C. Riedl, D. S. Lee, B. Krauss, L. Patthey, K. von Klitzing, J. H. Smet and U. Starke, *Phys. Rev. B.* 2010, **81**, 235401.

RSC Advances Accepted Manuscript

24 Y. Shi, J. K. Huang, L. Jin,Y.-T. Hsu, S. F. Yu, L.J. Li and H. Y. Yang, *Scientific Reports.* 2013, **3**, 1839.

25 U. Bhanu, M. R. Islam, L. Tetard and S. I. Khondaker, *Scientific Reports.* 2014, **3**, 5575.

26 K. S. Novoselov, D. Jiang, F. Schedin, T. J. Booth, V. V. Khotkevich, S. V. Morozov and A. K. Geim, *PNAS,* 2005, **102**, 10451–10453.

27 C. Lee, H. Yan, L. E. Brus, T. F. Heinz, J. Hones and S. Ryu, *ACS Nano letters*, 2010, **4**, 2695-2700.

28 B. Chakraborty, A. Bera, D. V. S. Muthu, S. Bhowmick, U. V. Waghmare and A. K. Sood, *Physical Review B.* 2012, **85**, 161403.

29 M. Buscema, G. A. Steele, H. S. J. V. Zant and A. Castellanos-Gomez, *Nano Research, Springer.* 2014, **7**, 1-11.

30 H. Nan, Z. Wang, W. Wang, Z. Liang, Y. Lu, Q. Chen, D. He, P. Tan, F. Miao, X. Wang, J. Wang and Z. Ni, *ACS Nano*., 2014**, 8**, 5738–5745.

31 Q. Li, Y. Jiang, R. Han, X. Zhong, S. Liu, Z. Y. Li, Y. Sha and D. Xu, *Small, Wiley,* 2013, **9**, 927-932.

32 S. R. Emory, W. E. Haskins and S. Nie, *J. Am. Chem. Soc.,* 1998, **120**, 8009−8010.

33 H. Xu, J. Aizpurua, M. Käll and P. Apell, *Phys. Rev. E*, 2000, **62**, 4318−4324.

34 H. Xu, E. J. Bjerneld, M. Käll and L. Börjesson, *Phys. Rev. Lett.,* 1999, **83**, 4357−4360.

35 M. Moskovits, *J. Raman Spectrosc.,* 2005, **36**, 485−496.

36 K. A. Bosnick, J. Jiang and L. E. Brus, *J. Phys. Chem. B,* 2002, **106**, 8096−8099.

37 A. Otto, *J. Raman Spectrosc.,* 2002**, 33**, 593−598.

RSC Advances Accepted Manuscript

38 J. P. Camden, J. A. Dieringer, Y. Wang, D. J. Masiello, L. D. Marks, G. C. Schatz and R. P. Van Duyne, *J. Am. Chem. Soc.,* 2008, **130**, 12616−12617.

39 L. Yang, B. Yan, W. R. Premasiri, L. D. Ziegler, L. D. Negro and B. M. Reinhard, *Adv. Funct. Mater.* 2010**, 20**, 2619−2628.

40 M. Moskovits, *Rev. of Mod. Phy.* 1985**,** 57, **3**, 783−826.

41 A. M. Michaels, J. Jiang and L. Brus, *J. Phys. Chem. B,* 2000**, 104**, 11965−11971.

42 Z.-Q. Tian, B. Ren and D.-Y. Wu, *J. Phys. Chem. B*, 2002**, 106**, 9463−9483.

43 A. Tao, F. Kim, C. Hess, J. Goldberger, R. He, Y. Sun, Y. Xia and P. Yang, *Nano Lett.***,** 2003*,* **3**, 1229−1233.

44 K. A. Willets and R. P. V. Duyne, *Annu. Rev. Phys. Chem.,* 2007**, 58**, 267−297.

45 F. Le, D. W. Brandl, Y. A. Urzhumov, H. Wang, J. Kundu, N. J. Halas, J. Aizpurua and P. Nordlander, *ACS Nano,* 2008**, 2**, 707−718.

46 F. J. G.- Vidal and J. B. Pendry, *Phys. Rev. Lett.,* 1996, **77**, 1163−1166.

47 S. J. Tan, M. J. Campolongo, D. Luo and W. Cheng, *Nat. Nanotech.,* 2011**, 6**, 268.

48 S. Pal, R. Varghese, Z. Deng, Z. Zhao, A. Kumar, H. Yan and Y. Liu, *Angew. Chem. Int. Ed.,* 2011, **50**, 4176.

49 W. Guo, J. Yuan, Q. Dong and E. Wang, *J. Am. Chem. Soc., 2010,* **132**, 932.

50 A. V. Gourine, E. Llaudet, N. Dale and K. M. Spyer, *Nature,* 2005**, 436**, 108-111.

51 L. Berti and G. A. Burley, *Nat. Nanotech.*, 2008, **3**, 81-87.

RSC Advances Accepted Manuscript

52 D. Majumdar, A. Singha, P. K. Mondal and S. Kundu, *ACS Appl. Mater. Inter.,* 2013, **5**, 7798-7807.

53 G. Lu, H. Li, C. Liusman, Z. Yin, S. Wua and H. Zhang, *Chem. Sci.,* 2011, **2**, 1817-1821.

54 L. Jensen and G. C. Schatz, *J. Phys. Chem. A,* 2006**,** 110, **18**, 5973-5977.

RSC Advances Accepted Manuscript

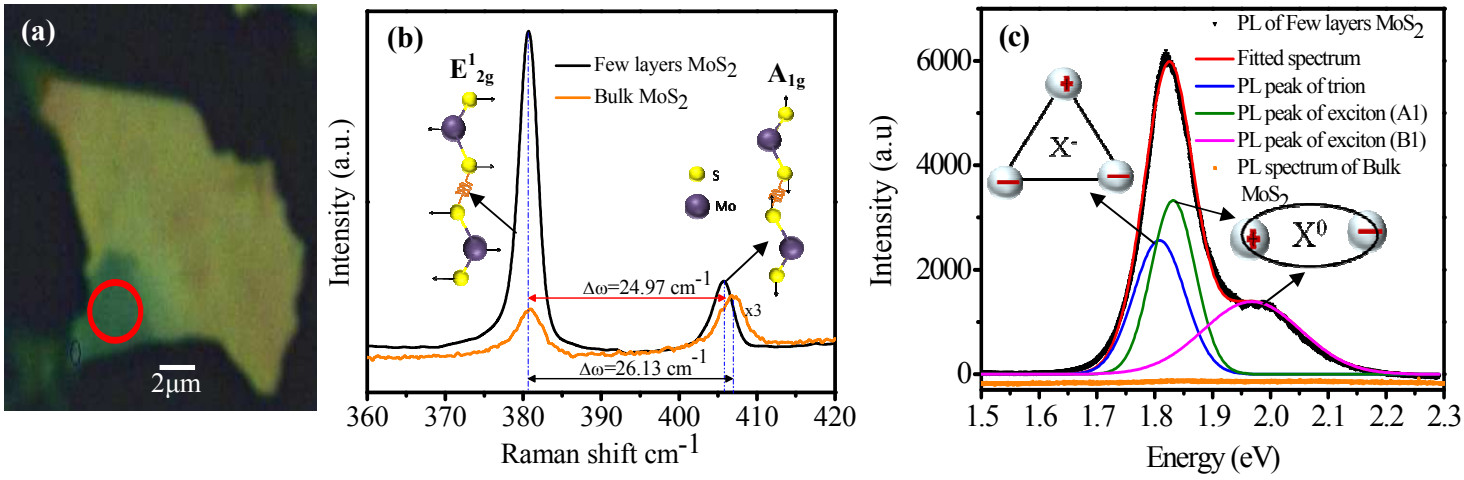

Figure 1: (a) Optical microscope image of few layers MoS_2. The measurements have been done at the place marked by red circle. (b) Raman spectrum of bulk (orange curve) and few layers (black curve) MoS_2. The schematic structure of the atomic displacements of the E^1_{2g} and A_{1g} are shown in the inset of the figure. (c) PL spectrum of bulk (orange curve) and few layers (black curve) MoS_2.The red line is the result of a fit to the experimental data of few layers MoS_2 with three Gaussians functions for X^- (blue), A1 (green), and B1 (magenta). The schematic structure of trion and exciton are shown in the inset

RSC Advances Accepted Manuscript

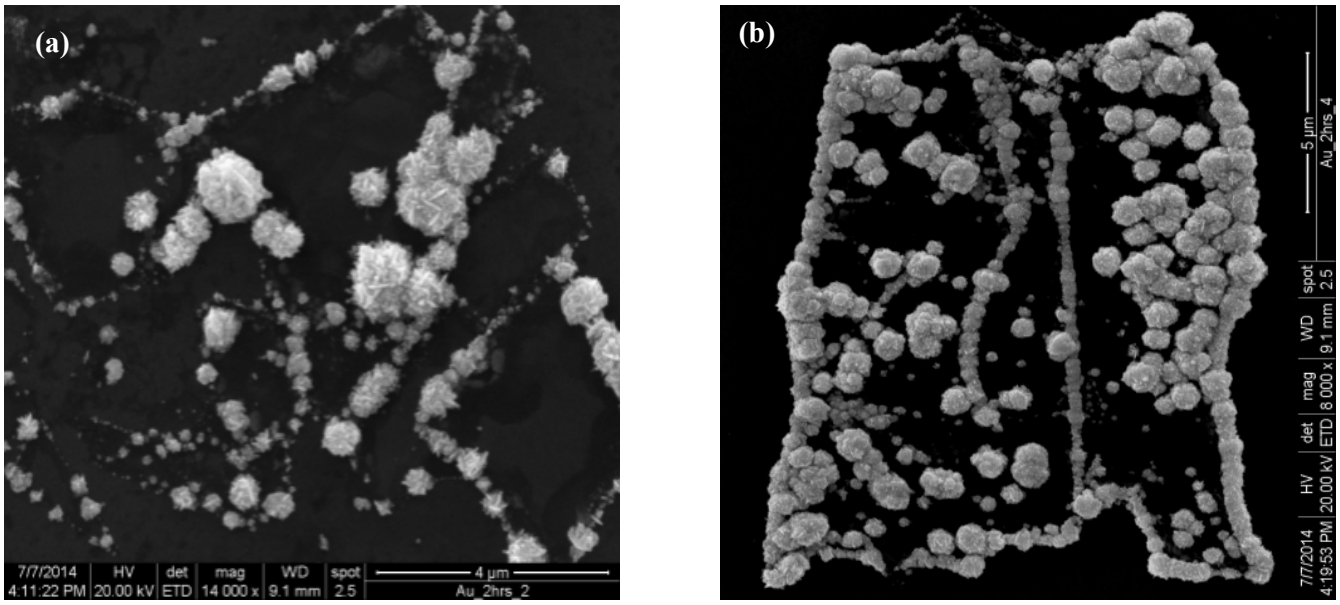

Figure 2: SEM images of (a) Sample S2 (b) Sample S4

RSC Advances Accepted Manuscript

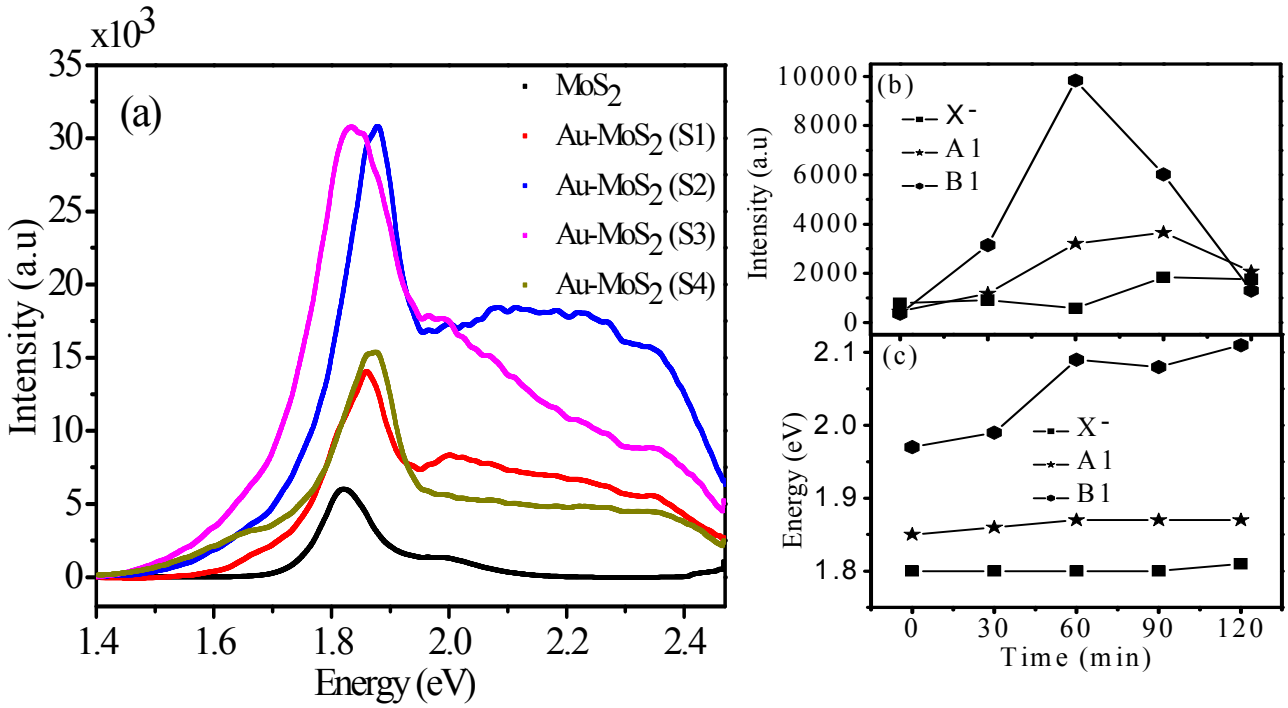

Figure 3: (a) PL spectra of few layers MoS_2 obtained at different dipping time [S1 (30 min), S2 (60 min), S3 (90 min) and S4 (120 min)] inside the $HAuCl_4$ solution. (b) Intensity and (c) energy of X^-, A1 and B1 peaks as a function of dipping time.

RSC Advances Accepted Manuscript

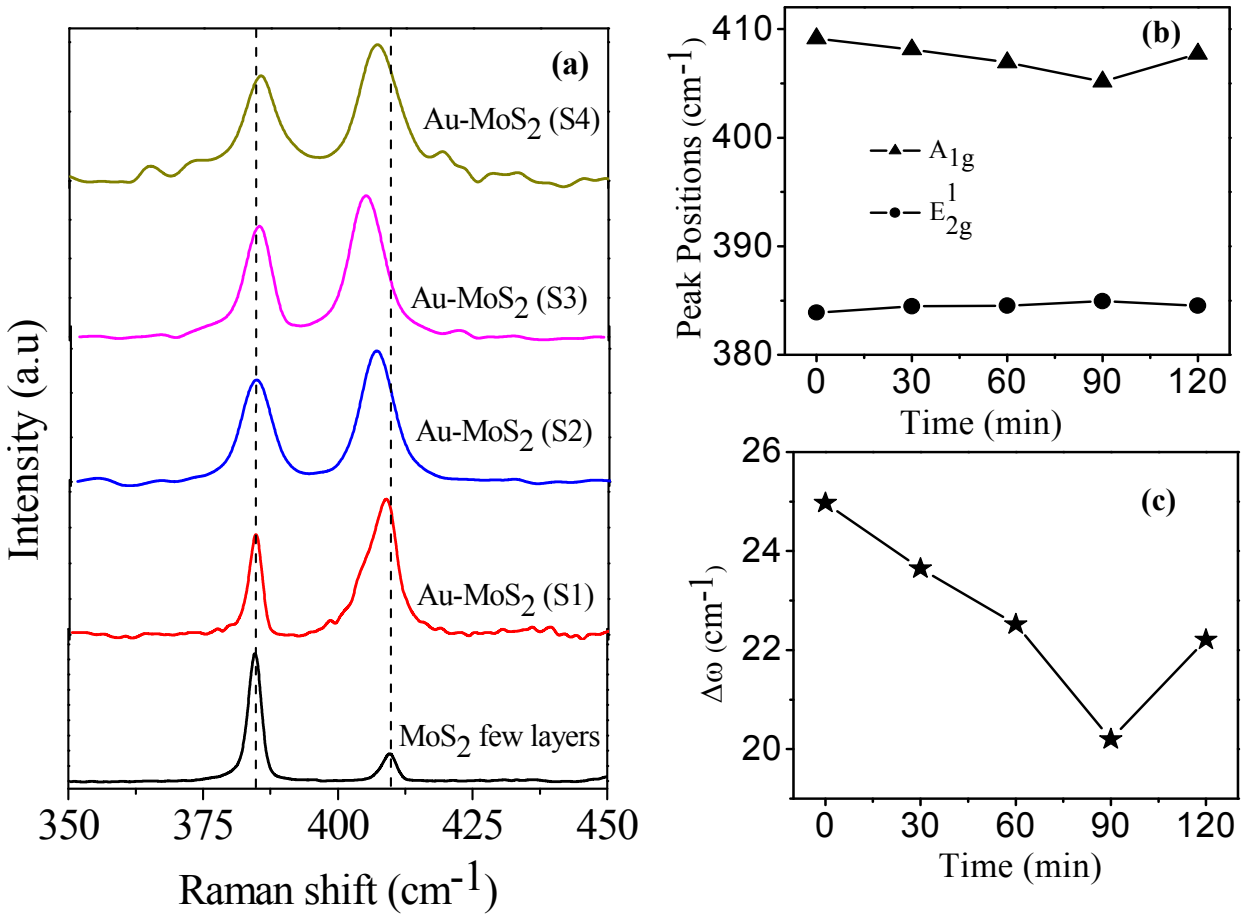

Figure 4: (a) Raman spectra of few layers MoS_2 obtained at different dipping time [S1 (30 min), S2 (60 min), S3 (90 min) and S4 (120 min)] inside the $HAuCl_4$ solution. (b) variation of E^1_{2g} and A_{1g} peaks positions as a function of dipping time (c) gap between E^1_{2g} and A_{1g} modes as a function of dipping time.

RSC Advances Accepted Manuscript

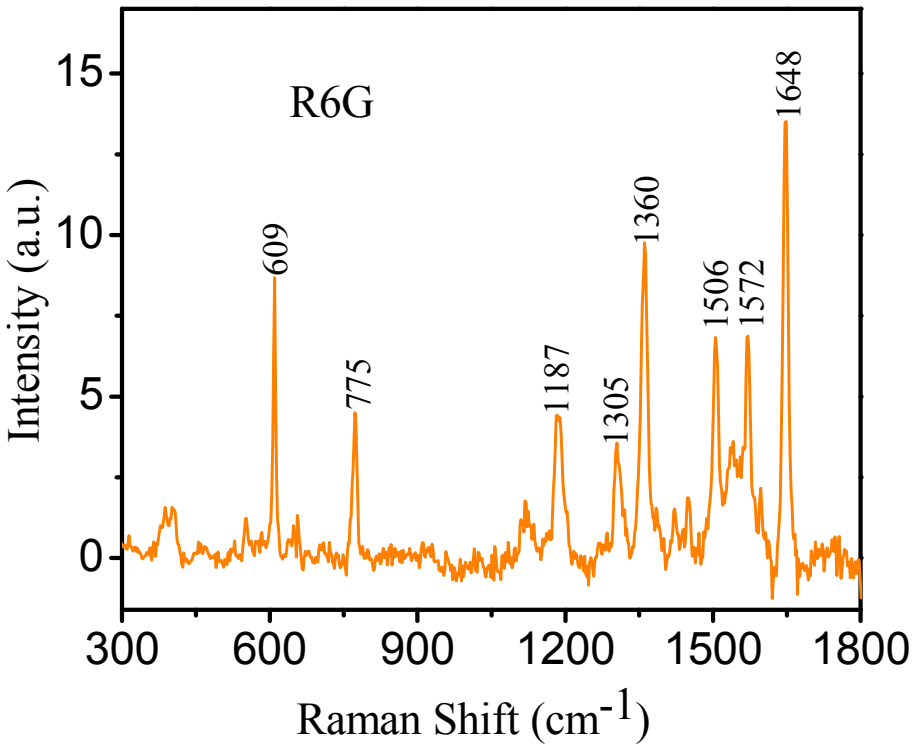

Figure 5: Raman spectrum of solid R6G dye. The characteristic peaks of R6G are assigned.

RSC Advances Accepted Manuscript

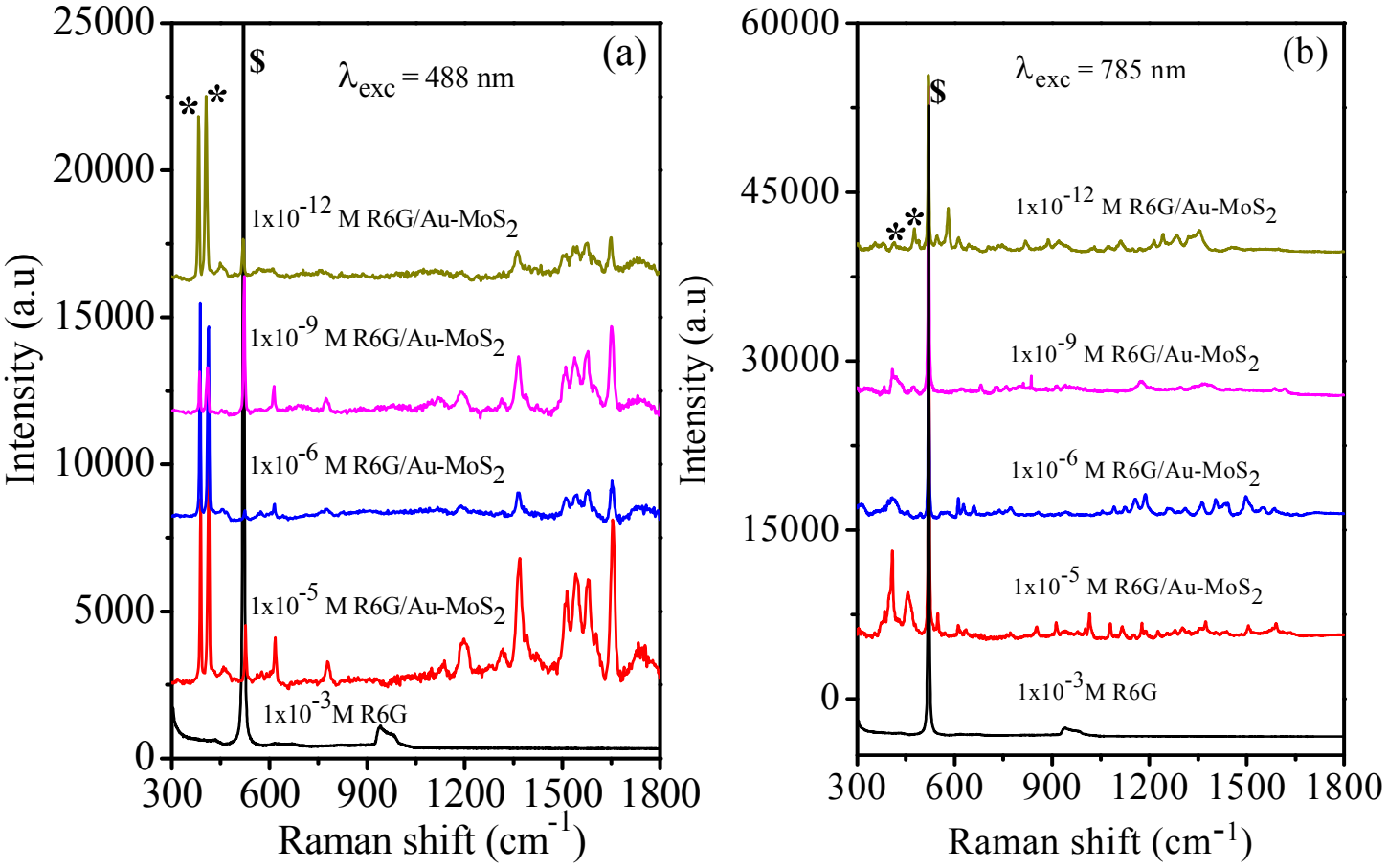

Figure 6: Raman spectra of 1 mM R6G solution (black) SERS spectra of R6G at concentrations of 1×10^{-5} M (red), 1×10^{-6} M (blue), 1×10^{-9} M (magenta), 1×10^{-12} M (dark yellow) with excitation wavelength (a) 488 nm and (b) 785 nm. The asterisk (*)-marked peaks are from MoS_2 and $ marked peak is from the Si substrate.

RSC Advances Accepted Manuscript

Table of Contents

Tuning of Photoluminescence Properties and Ultrasensitive Trace Detection in Few Layers MoS_2 by the Decoration of Gold Nanoparticles

Shib Shankar Singha, Dipanjan Nandi, Achintya Singha*

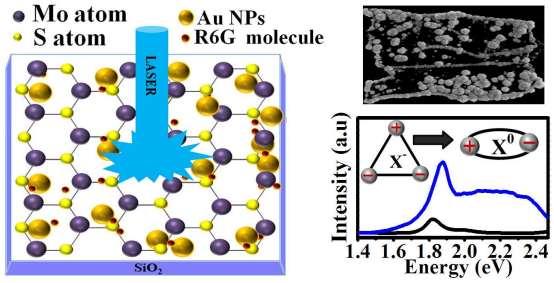

Tuning optical properties and ultrasensitive molecular detection by Au nanoparticles ornamented MoS_2.

RSC Advances Accepted Manuscript

RSC Advances Accepted Manuscript